



Published in final edited form as:

Cornea. 2016 November ; 35(11): 1471–1477. doi:10.1097/ICO.0000000000000948.

Needle Depth and Big Bubble Success in Deep Anterior Lamellar Keratoplasty: An Ex Vivo Microscope-Integrated OCT Study

Neel D. Pasricha, BA¹, Christine Shieh, MD¹, Oscar M. Carrasco-Zevallos, BS², Brenton Keller, BS², David Cunefare, BS², Jodhbir S. Mehta, FRCOphth, FRCS (Ed)^{3,4}, Sina Farsiu, PhD^{2,1}, Joseph A. Izatt, PhD^{2,1}, Cynthia A. Toth, MD^{1,2}, and Anthony N. Kuo, MD¹

¹Department of Ophthalmology, Duke University School of Medicine, Durham, NC, United States

²Department of Biomedical Engineering, Duke University, Durham, NC, United States

³Singapore National Eye Centre, Singapore

⁴Duke-NUS Graduate Medical School, Singapore

Abstract

Purpose—To examine big bubble (BB) formation success rates in deep anterior lamellar keratoplasty (DALK) at various corneal depths using real-time guidance from swept-source microscope-integrated optical coherence tomography (SS-MIOCT).

Methods—The DALK procedure was performed ex vivo with 34 human donor corneoscleral buttons on pressurized artificial anterior chambers using Anwar and Teichmann's BB technique. We inserted a needle under controlled ex vivo conditions to corneal depths ranging from 40–90+% using real-time guidance from SS-MIOCT and injected air. BB success was then determined for each injection.

Results—The average needle depth for successful full BB formation was 79.9±3.0% compared to 66.9±2.6% for partial BB formation and 49.9±3.4% for no BB formation ($P<.0001$). Expressed as stroma below the needle tip, this corresponded to 123.9±20.0 μm for successful full BB formation compared to 233.7±23.8 μm for partial BB formation and 316.7±17.3 μm for no BB formation ($P<.0001$). All other variables tested (gender, race, age, endothelial cell density, air injected, needle angle, and central corneal thickness) did not significantly affect BB formation success rates.

Conclusions—BB formation in DALK is more successful if needle insertion and air injection occur at deeper corneal depth. However, 90+% corneal depth was not necessary in this ex vivo model of DALK. SS-MIOCT can be used to accurately guide the needle in real-time.

Keywords

OCT; DALK; big bubble

Corresponding Author: Anthony N. Kuo, Duke Eye Center, DUMC Box 3802, Durham, NC 27710. anthony.kuo@duke.edu. Phone: 919-684-5769. Fax: 919-681-7661.

Conflicts of Interest

For the remaining authors no conflicts of interest were declared.

INTRODUCTION

Deep anterior lamellar keratoplasty (DALK) is an alternative to penetrating keratoplasty (PK) for the treatment of keratoconus and corneal stromal diseases in patients with healthy endothelium that is gaining popularity worldwide.¹⁻³ Unlike PK, DALK preserves the host endothelium and thus eliminates the risk of endothelial rejection, reduces the required duration of corticosteroid therapy, and leads to more rapid wound healing.⁴⁻⁸ Visual acuity in both PK and DALK are similar, but only if the dissection into the posterior stroma is sufficiently deep in order to prevent the development of tissue interface scarring between the donor cornea and recipient stromal tissue.¹⁰⁻¹³ There are numerous techniques to help bare DM, including hydrodelamination, viscoelastic dissection, and anterior chamber air injection. The one that most surgeons prefer is the big bubble (BB) technique, first described by Anwar and Teichmann¹⁴ in 2002, which uses a deep intrastromal air injection to dissect between DM and the overlying corneal stroma.

To perform the BB technique, many surgeons believe the needle must be inserted as close as possible to DM (which could be interpreted as 90+% corneal depth) without penetrating into the anterior chamber prior to injecting air.¹⁵⁻¹⁷ This is technically challenging and explains the steep learning curve and low success rates associated with DALK.^{1,6,15,18} A previous study by Scorcia et al¹⁹ used intraoperative anterior segment (AS) optical coherence tomography (OCT) to show a significant difference between needle depth and BB success, but it did so by imaging the needle tract rather than imaging the needle insertion in real-time. Additionally, the previous study had the surgeon attempt to maneuver the needle to “a plane thought to be deep enough” rather than test BB success at a range of corneal depths. Until now, no study has examined the real-time guidance of needle insertion to various corneal depths to determine the effect of needle depth on BB success in DALK. Performing such a variable needle depth study in live surgery presents a problem from an ethical standpoint as it would be difficult to have surgeons purposely aim for shallow corneal depths given the current convention that significant corneal depth may be necessary for BB success. Also, an ex vivo setting helps control inter-patient variability. Hence, we used an ex vivo setting both to intentionally allow a range of needle depths and to control for variables such as “intraocular” pressure and needle angle. Finally, swept-source microscope-integrated OCT (SS-MIOCT) was used to actively guide the needle in real-time to varying corneal depths ranging from 40–90+% prior to injecting air to determine BB success as a result of needle depth.

MATERIALS & METHODS

This single center experimental study used 34 research grade human corneoscleral buttons obtained from our local eye bank (Miracles in Sight, Winston-Salem, NC, USA). Exclusion criteria were previous corneal surgery, presence of traumatic scars, and more than 7 days since donor's death. Duke University Health System Institutional Review Board (IRB) approval was obtained and we adhered to the tenets of the Declaration of Helsinki.

4D Swept-Source Microscope-Integrated OCT

The sample arm optics of our MIOCT system has been reported in a previous publication.²⁰ Briefly, a customized mechanical enclosure allowed seamless integration of a MIOCT system capable of 3D imaging across time (4D) into a Leica M844 ophthalmic surgical microscope (Leica Microsystems, Buffalo Grove, IL), ensured parfocality of the two systems, and allowed for concurrent MIOCT and surgical microscope use. The system used a SS-OCT engine with a swept frequency source centered at 1040 ± 50 nm (Axsun Technologies, Billerica, MA) and the following imaging parameters: A-scan rate – 100 kHz, sensitivity – 102 dB, imaging range – $12\times 12\times 7.4$ mm (lateral [x,y] and depth [z]), resolution – $14\times 14\times 7.8$ μ m. The volumetric imaging rate of the 4D SS-MIOCT system depended on the acquisition sampling density. Our protocol of 500 A-scans/B-scan and 100 B-scans/volume used in this study yielded a rate of 2 volumes/second. Custom tracking hardware to move the OCT scan location in real-time was also employed. The system software was custom written in C++ and used graphics processing unit (GPU)-based processing that incorporated live recording to continuously save each volumetric dataset, thus enabling continuous 4D SS-MIOCT recording of the needle injection. The 4D SS-MIOCT images were acquired, processed, rendered, and displayed in real-time on a monitor to allow the MIOCT technician to help verbally guide the surgeon's needle to the target needle depth (Supplemental Digital Content 1, video showing 4D SS-MIOCT guidance of the needle in real-time).

Surgical Procedure

We performed ex vivo DALK with the same surgeon (C.S.) using Anwar and Teichmann's BB technique in the following manner. The corneoscleral buttons were loaded onto a Barron artificial anterior chamber (Katena, Denville, NJ) connected by tubing to a 10 mL syringe filled with balanced salt solution (BSS). We maintained a 30 cm BSS column height for all testing to provide a consistent and physiologic level of "intraocular" pressure equivalent to approximately 22 mm Hg in the eye, which was verified as physiologic using a Tono-Pen XL (Medtronic, Minneapolis, MN) (Supplemental Digital Content 2, picture showing ex vivo setup). After trephining to approximately 50% corneal depth using an 8.0 mm Barron radial vacuum trephine, a 27-gauge needle bent approximately 60° with the bevel facing downward and attached to a 5 mL syringe was inserted into the stroma from the trephination site at a similar angle of approach for each injection and advanced into the paracentral cornea under SS-MIOCT guidance to one of three target needle depths: 50% (target needle depth 1), 70% (target needle depth 2), and 90% (target needle depth 3). We randomly selected one of the three target needle depths for each injection while ensuring a comparable number of injections at each target needle depth. This block randomization method was employed to mitigate the potential influence of increasing experience on the surgeon's ability to accurately achieve a specific target needle depth. Once the surgeon was thought to be at the selected target needle depth, she injected air until either a sudden ease of resistance on the plunger was felt and a classic "explosive" appearance of a white, semi-opaque disk was noted or until a dense white opacity extended peripherally to the trephination groove.

Determining Big Bubble Success

In many cases, the corneal emphysema resulting from the air injection caused significant opacification, making BB success determination difficult from the standard top down, epithelium side up, view. To be absolutely certain of our BB formation result, we removed the corneoscleral button from the artificial anterior chamber and turned the button endothelial side up to visually confirm the presence of a centrally located air bubble spanning at least 7 mm in diameter (full BB), a single bubble less than 7 mm in diameter or multiple smaller bubbles (partial BB), or no bubble (no BB). We chose 7 mm diameter as the cutoff point for successful full BB formation to include only those bubbles almost spanning the full 8.0 mm trephination diameter and larger. Figure 1 shows SS-MIOCT images from a sample in the full and partial BB formation groups.

Central Corneal Thickness and Needle Depth Measurements

As described earlier, we recorded 4D SS-MIOCT images of each needle injection in real-time. The SS-MIOCT volume prior to needle insertion was used to analyze central corneal thickness (CCT). From this volume, the B-scan (2D) image over the central cornea was selected. Distortions in the B-scan introduced by refraction were removed in post-processing with MATLAB (MathWorks, Natick, MA, USA).²¹ For the refraction correction, a corneal group refractive index of 1.384 was used based on calculations for a 1040 nm center wavelength.^{22,23} The epithelium and endothelium at the central corneal location were manually segmented. From this, the CCT was then calculated.

To calculate needle depth and needle angle, the previous steps were repeated using the SS-MIOCT volume immediately prior to air injection. From this volume, the B-scan (2D) image with the needle tip was selected. The needle tip position was manually segmented and the epithelium and endothelium were traced semi-automatically in MATLAB. The stroma above the needle, stroma below the needle, and needle depth percentage were then calculated (Fig 2). Separately, PixelStick (Plum Amazing, Princeville, HI, USA) was used to measure the needle angle, with zero degrees referring to the horizontal image plane.

Statistical Analysis

Statistical analyses were performed using JMP statistical software (SAS Institute, Cary, NC, USA). The numbers for gender and race and means for age, endothelial cell density (ECD), air injected, needle angle, CCT, stroma below needle, and needle depth percentage were compared for the 3 BB formation groups. A chi-square test was used for our nominal variables (gender and race) and a one-way analysis of variance (ANOVA) was used for our continuous variables. Statistical significance was defined as a two-sided *P* value of <0.05. Each pair of means from significant variables on one-way ANOVA was compared using Student's *t* tests.

RESULTS

Twenty-three corneoscleral buttons came from male donors (67.6%) and 11 came from female donors (32.4%). Twenty-eight were from Caucasian donors (82.4%) and 6 were from African American donors (17.6%). The average age±standard error was 60.0±2.2 years and

2557±107 cells/mm² for ECD. Our ex vivo corneas had an average±standard error CCT of 556.2±9.2 µm.

The average needle depth percentage±standard error for target needle depth 1 (50%) was 50.1±2.3% (range, 40.0–58.0%), for target needle depth 2 (70%) was 69.5±1.3% (range, 62.0–74.9%), and for target needle depth 3 (90%) was 87.7±1.7% (range, 82.2–97.6%). Corneal perforations occurred during needle insertion in 2 injections while aiming for target needle depth 3 and were excluded from the analysis. Figure 3 shows the rate of BB formation at each of the three targeted needle depths. Successful full BB formation only occurred in 1 out of 10 injections at target needle depth 1, whereas 5 out of 12 injections resulted in successful full BB formation at target needle depth 2. All 10 out of 10 injections at target needle depth 3 resulted in successful full BB formation, excluding the 2 in which corneal perforation occurred.

Of the 32 injections without corneal perforation, 16 (50%) resulted in successful full BB formation, 8 (25%) resulted in partial BB formation, and 8 (25%) resulted in no BB formation. As shown in Figure 4, in the successful full BB formation group, needle depth percentage (mean, 79.9±3.0%) was significantly higher ($P<0.0001$) than that recorded in the partial BB formation group (mean, 66.9±2.6%) and the no BB formation group (mean, 49.9±3.4%). Similarly, stroma below needle was significantly lower ($P<0.0001$) in the successful full BB formation group (mean, 123.9±20.0 µm) compared to both the partial BB formation group (mean, 233.7±23.8 µm) and the no BB formation group (mean, 316.7±17.3 µm).

No further significant differences were noted between the 3 BB formation groups in terms of gender ($P=0.16$), race ($P=0.08$), age ($P=0.10$), ECD ($P=0.37$), air injected ($P=0.06$), needle angle ($P=0.93$), or CCT ($P=0.11$). Table 1 lists the baseline characteristics and needle insertion measurements recorded.

DISCUSSION

To date, no study has tested the effect of needle depth on BB success by injecting air at a range of corneal depths and then determining BB success. Furthermore, no study has used intraoperative imaging to guide the needle in real-time to a target needle depth. In this study, we used SS-MIOCT to guide a needle in real-time to corneal depths ranging from 40–90% prior to injecting air and then determining BB success in a controlled, ex vivo setting for this purpose. Based on our results, it was determined that the mean needle depth percentage for successful full BB formation was significantly higher (79.9±3.0% vs. 66.9±2.6% vs. 49.9±3.4%; $P<0.0001$) than for partial and no BB formation groups. Additionally, we determined that SS-MIOCT can accurately guide the needle to a target needle depth within ±10%, as shown by the range of corneal depths achieved for each of our 3 target needle depths.

We had 2 corneal perforations despite SS-MIOCT guidance. This corresponds to a 5.9% perforation rate across all needle injections (2/34) and 16.7% in needle injections while aiming for the deepest target needle depth of 90% (2/12). A recent study by Busin et al²⁴

compared reported perforation rates during the DALK procedure from 10 papers published between 2010–2015 and found a range of 4–31.8%. Considering the surgeon in our study was a first-year cornea fellow new to the DALK procedure, our perforation rate is comparable and potentially even better than expected. In the future, technologies that enable micrometer-scale precision of surgical instruments to match the micrometer-scale visualization provided by SS-MIOCT may be necessary to fully utilize the potential of SS-MIOCT.

Since our study aimed to test BB success at a range of corneal depths, rather than only deep corneal depths, we required an ex vivo setting. Conducting an in vivo study testing corneal depths as shallow as 40% would not be feasible since our results show successful full BB formation occurred at an average needle depth percentage of $79.9 \pm 3.0\%$. Although an ex vivo setting was necessary for this study to intentionally vary and test the effect of needle depth, we realize that it does not completely recreate DALK surgery in a person. Also, all of our tested corneas were relatively normal thickness, and thinner corneas, as seen in keratoconus, may offer less choice in needle placement depth. Furthermore, our tested corneas were free of any scar tissue, which may be present in some corneal transplant patients and can potentially affect big bubble formation. However, the ex vivo setting does afford several advantages over an in vivo setting, namely control of other variables. This included allowing us to control “intraocular” pressure by maintaining a constant column height that provided a normal physiologic pressure for all injections. Additionally, controlling needle angle across all injections was simplified ex vivo.

No significant difference was recorded for gender, race, age, ECD, air injected, needle angle, or CCT between the 3 BB formation groups. Of note, the diabetic status of donors, which appears to be a significant variable in DM baring for the preparation of Descemet’s membrane endothelial keratoplasty (DMEK) tissue, was unavailable and is thus an uncontrolled variable in our study.²⁵ Our CCT measurements were comparable for healthy patients but thicker than would be expected for keratoconus patients. However, thicker or thinner CCT values did not significantly affect BB formation in our study and in other studies (Touhami S et al. IOVS 2015;405:ARVO E-Abstract 3973 and Scorcia et al¹⁹). More air was injected for the partial and no BB formation groups compared to the full BB formation group, eliminating the possibility that simply injecting more air in these cases could create a full BB. The rate at which air was injected was difficult to quantify and may have played a role in BB formation success. However, having the same surgeon (C.S.) perform all injections helped decrease any inter-surgeon variability in this and other DALK BB technique parameters.

Interestingly, a full BB was achieved at needle depth percentages as shallow as 58.0%, 62.0%, and 62.1% in three cases. This provides evidence that other variables besides needle depth percentage may contribute to BB success. All injections shallower than 55.2% corneal depth were unsuccessful, resulting in no BB formation. Needle depth percentages deeper than 67.6% resulted in either partial or full BB formation, and those deeper than 74.9% resulted in only full BB formation. Since the only 2 corneal perforations we experienced in this study occurred while aiming for our deepest target needle depth of 90%, this suggests that corneal surgeons could aim for a target needle depth of 80% to maximize the rate of

successful full BB formation and minimize the risk of corneal perforation. Even if PK conversion is not needed, corneal perforation in the DALK procedure has been shown postoperatively to result in higher ECD loss and worse visual outcomes.⁵ Using a blunt cannula, as opposed to a needle, can provide an additional safety measure against corneal perforation.²⁶

A study by Scorcia et al¹⁹ used AS OCT of the needle tract formed during in vivo DALK BB procedures and found that the average distance between the cannula tip and DM for successful BB formation was $90.4 \pm 27.7 \mu\text{m}$ and $136.7 \pm 24.2 \mu\text{m}$ for unsuccessful BB formation. Our study found more stroma below the needle than this for both the full and no BB groups ($123.9 \pm 20.0 \mu\text{m}$ and $316.7 \pm 17.3 \mu\text{m}$, respectively). One reason for this discrepancy is that the Scorcia et al study had the surgeon perform needle injections at only deep corneal depths whereas our study had the surgeon perform needle injections at a range of corneal depths. Another possible explanation is that the relative depth, as opposed to the absolute depth, is the more important variable. The corneas in the Scorcia et al study were significantly thinner (average preoperative thinnest point of $373.1 \pm 86.2 \mu\text{m}$) compared to our corneas (average CCT of $556.2 \pm 9.2 \mu\text{m}$). Interestingly, this means the Scorcia et al study had an average cannula depth percentage of 75.8% ($282.7/373.1$) for successful BB formation, assuming the cannula tip was at the preoperative thinnest point of the cornea. This compares closely to our reported average needle depth percentage of 79.9% for successful BB formation. A recent study by Steven et al²⁷ used spectral-domain (SD) OCT integrated into the microscope to image 6 in vivo DALK cases in real-time. However, their SD-OCT system could only acquire 2D images and thus required constantly aligning the OCT-beam, making real-time guidance more challenging.

Some studies have classified the type of BB that forms based on anatomy, with Type-1 BB described as a well-circumscribed, central dome-shaped elevation up to 8.5 mm in diameter that forms at the deep stroma near DM and Type-2 BB described as a thin-walled, large BB of up to 10.5 mm in diameter that forms at the stromal-DM interface.^{16,28,29} Our study instead chose to look at BB type based on size, with full BB describing a single, centrally located bubble of 7 mm in diameter or larger, partial BB describing a single bubble smaller than 7 mm in diameter or multiple smaller bubbles, and no BB describing the complete absence of any bubble. We did this because clinically, our distinction of full, partial, or no BB formation determines the next step of the DALK procedure. In cases of no BB formation, the surgeon may choose to attempt needle reinsertion and air injection at a different site whereas in partial BB formation, the surgeon may choose to expand the dissection plane by other means, such as viscoelastic injection.³⁰ For the full BB formation group, stromal dissection can continue as planned.

Our results demonstrate the use of SS-MIOCT in achieving a sufficiently deep needle depth to create a full BB during DALK. A further step forward could be made if the current metallic surgical instruments were replaced with OCT-transparent surgical instruments.³¹ This would reduce the shadowing effect seen directly under the needle in SS and SD-OCT systems.³² Fortunately, in our study the endothelium ahead of the needle tip was easily visualized and allowed for accurate forward needle guidance and depth measurements. Although our SS-MIOCT system allowed for simultaneous surgery and imaging, it still

required a technician to maintain proper alignment of the B-scan parallel to the needle. Having automatic tool tracking integrated into the SS-MIOCT software would free the technician of this responsibility. With future advancements in heads-up display (HUD) technology, the SS-MIOCT data may be projected into the microscope oculars, giving surgeons direct access to both the surgical field and the SS-MIOCT information through the same view with the ability for surgeons to control the SS-MIOCT imaging location.^{33–35} Our ex vivo model combined with SS-MIOCT and HUD technology could serve as a valuable training platform for corneal surgeons. Despite the lack of HUD technology in this study, the surgeon was still able to reach $\pm 10\%$ of the target needle depth using verbal feedback from the MIOCT technician.

To the best of our knowledge, this study is among the first to directly test BB success at varying corneal depths during DALK, using an ex vivo model to show that $<90\%$ needle depth can achieve successful full BB formation. No other study to date has used SS-MIOCT to actively guide in real-time the needle injection for the BB technique. As this technology gains increasingly widespread use, its utility in DALK and other AS surgeries will become more clear.³⁶

Supplementary Material

Refer to Web version on PubMed Central for supplementary material.

Acknowledgments

Source of Funding: At the time of this work, Dr. Izatt was Chairman and Chief Scientific Advisor for Bioptigen Inc. (since acquired by Leica Microsystems), and had corporate, equity, and intellectual property interests (including royalties) in this company. Dr. Toth receives financial support from Alcon, Bioptigen, and Genentech and has an intraoperative imaging patent with Duke University. Dr. Farsiu has an imaging segmentation patent with Duke University. Dr. Kuo has an imaging algorithm patent licensed by Duke to Bioptigen, which is unrelated to the present work.

We would like to thank Miracles in Sight (Winston-Salem, NC) for graciously providing us with all the human corneoscleral buttons used in this study.

REFERENCES

1. Feizi S, Javadi MA, Jamali H, et al. Deep anterior lamellar keratoplasty in patients with keratoconus: big-bubble technique. *Cornea*. 2010; 29:177–182. [PubMed: 20023579]
2. Awan MA, Roberts F, Hegarty B, et al. The outcome of deep anterior lamellar keratoplasty in herpes simplex virus-related corneal scarring, complications and graft survival. *Br J Ophthalmol*. 2010; 94:1300–1303. [PubMed: 20554507]
3. Noble BA, Agrawal A, Collins C, et al. Deep Anterior Lamellar Keratoplasty (DALK): visual outcome and complications for a heterogeneous group of corneal pathologies. *Cornea*. 2007; 26:59–64. [PubMed: 17198015]
4. Borderie VM, Sandali O, Bullet J, et al. Long-term results of deep anterior lamellar versus penetrating keratoplasty. *Ophthalmology*. 2012; 119:249–255. [PubMed: 22054997]
5. Cheng YY, Visser N, Schouten JS, et al. Endothelial cell loss and visual outcome of deep anterior lamellar keratoplasty versus penetrating keratoplasty: a randomized multicenter clinical trial. *Ophthalmology*. 2011; 118:302–309. [PubMed: 20832121]
6. Fontana L, Parente G, Tassinari G. Clinical outcomes after deep anterior lamellar keratoplasty using the big-bubble technique in patients with keratoconus. *Am J Ophthalmol*. 2007; 143:117–124. [PubMed: 17188045]

7. Han DC, Mehta JS, Por YM, et al. Comparison of outcomes of lamellar keratoplasty and penetrating keratoplasty in keratoconus. *Am J Ophthalmol.* 2009; 148:744.e1–751.e1. [PubMed: 19589495]
8. Romano V, Iovieno A, Parente G, et al. Long-term clinical outcomes of deep anterior lamellar keratoplasty in patients with keratoconus. *Am J Ophthalmol.* 2015; 159:505–511. [PubMed: 25486540]
9. Funnell CL, Ball J, Noble BA. Comparative cohort study of the outcomes of deep lamellar keratoplasty and penetrating keratoplasty for keratoconus. *Eye (Lond).* 2006; 20:527–532. [PubMed: 15877089]
10. Abdelkader A, Kaufman HE. Descemet's versus pre-descemet's lamellar keratoplasty: clinical and confocal study. *Cornea.* 2011; 30:1244–1252. [PubMed: 21955636]
11. Reinhart WJ, Musch DC, Jacobs DS, et al. Deep anterior lamellar keratoplasty as an alternative to penetrating keratoplasty a report by the american academy of ophthalmology. *Ophthalmology.* 2011; 118:209–218. [PubMed: 21199711]
12. Tan DT, Anshu A, Parthasarathy A, et al. Visual acuity outcomes after deep anterior lamellar keratoplasty: a case-control study. *Br J Ophthalmol.* 2010; 94:1295–1299. [PubMed: 20829318]
13. Ardjomand N, Hau S, McAlister JC, et al. Quality of vision and graft thickness in deep anterior lamellar and penetrating corneal allografts. *Am J Ophthalmol.* 2007; 143:228–235. [PubMed: 17258522]
14. Anwar M, Teichmann KD. Big-bubble technique to bare Descemet's membrane in anterior lamellar keratoplasty. *J Cataract Refract Surg.* 2002; 28:398–403. [PubMed: 11973083]
15. Bhatt UK, Fares U, Rahman I, et al. Outcomes of deep anterior lamellar keratoplasty following successful and failed 'big bubble'. *Br J Ophthalmol.* 2012; 96:564–569. [PubMed: 22133987]
16. Ghanem RC, Bogoni A, Ghanem VC. Pachymetry-Guided Intrastromal Air Injection ("Pachy-Bubble") for Deep Anterior Lamellar Keratoplasty: Results of the First 110 Cases. *Cornea.* 2015
17. Riss S, Heindl LM, Bachmann BO, et al. Pentacam-based big bubble deep anterior lamellar keratoplasty in patients with keratoconus. *Cornea.* 2012; 31:627–632. [PubMed: 22357390]
18. Smadja D, Colin J, Krueger RR, et al. Outcomes of deep anterior lamellar keratoplasty for keratoconus: learning curve and advantages of the big bubble technique. *Cornea.* 2012; 31:859–863. [PubMed: 22495029]
19. Scorcio V, Busin M, Lucisano A, et al. Anterior segment optical coherence tomography-guided big-bubble technique. *Ophthalmology.* 2013; 120:471–476. [PubMed: 23177365]
20. Tao YK, Ehlers JP, Toth CA, et al. Intraoperative spectral domain optical coherence tomography for vitreoretinal surgery. *Opt Lett.* 2010; 35:3315–3317. [PubMed: 20967051]
21. Westphal V, Rollins A, Radhakrishnan S, et al. Correction of geometric and refractive image distortions in optical coherence tomography applying Fermat's principle. *Opt Express.* 2002; 10:397–404. [PubMed: 19436373]
22. Zhao M, Kuo AN, Izatt JA. 3D refraction correction and extraction of clinical parameters from spectral domain optical coherence tomography of the cornea. *Opt Express.* 2010; 18:8923–8936. [PubMed: 20588737]
23. Lin RC, Shure MA, Rollins AM, et al. Group index of the human cornea at 1.3-microm wavelength obtained in vitro by optical coherence domain reflectometry. *Opt Lett.* 2004; 29:83–85. [PubMed: 14719668]
24. Busin M, Scorcio V, Leon P, et al. Outcomes of Air Injection within 2 mm inside a Deep Trephination for Deep Anterior Lamellar Keratoplasty in Eyes with Keratoconus. *Am J Ophthalmol.* 2016
25. Greiner MA, Rixen JJ, Wagoner MD, et al. Diabetes mellitus increases risk of unsuccessful graft preparation in Descemet membrane endothelial keratoplasty: a multicenter study. *Cornea.* 2014; 33:1129–1133. [PubMed: 25222000]
26. Sarnicola V, Toro P. Blunt cannula for descemet's deep anterior lamellar keratoplasty. *Cornea.* 2011; 30:895–898. [PubMed: 21464706]
27. Steven P, Le Blanc C, Lankenau E, et al. Optimising deep anterior lamellar keratoplasty (DALK) using intraoperative online optical coherence tomography (iOCT). *Br J Ophthalmol.* 2014; 98:900–904. [PubMed: 24590554]

28. Dua HS, Faraj LA, Said DG, et al. Human corneal anatomy redefined: a novel pre-Descemet's layer (Dua's layer). *Ophthalmology*. 2013; 120:1778–1785. [PubMed: 23714320]
29. Goweida MB. Intraoperative review of different bubble types formed during pneumodissection (big-bubble) deep anterior lamellar keratoplasty. *Cornea*. 2015; 34:621–624. [PubMed: 25909235]
30. Muftuoglu O, Toro P, Hogan RN, et al. Sarnicola air-visco bubble technique in deep anterior lamellar keratoplasty. *Cornea*. 2013; 32:527–532. [PubMed: 23187161]
31. Ehlers JP, Srivastava SK, Feiler D, et al. Integrative advances for OCT-guided ophthalmic surgery and intraoperative OCT: microscope integration, surgical instrumentation, and heads-up display surgeon feedback. *PLoS One*. 2014; 9:e105224. [PubMed: 25141340]
32. De Benito-Llopis L, Mehta JS, Angunawela RI, et al. Intraoperative anterior segment optical coherence tomography: a novel assessment tool during deep anterior lamellar keratoplasty. *Am J Ophthalmol*. 2014; 157:334.e3–341.e3. [PubMed: 24332371]
33. Ehlers JP, Kaiser PK, Srivastava SK. Intraoperative optical coherence tomography using the RESCAN 700: preliminary results from the DISCOVER study. *Br J Ophthalmol*. 2014; 98:1329–1332. [PubMed: 24782469]
34. Heindl LM, Siebelmann S, Dietlein T, et al. Future Prospects: Assessment of Intraoperative Optical Coherence Tomography in Ab Interno Glaucoma Surgery. *Curr Eye Res*. 2014:1–4.
35. Shen L, Carrasco-Zevallos O, Keller B, et al. Novel Microscope-Integrated Stereoscopic Heads-up Display for Intrasurgical OCT in Ophthalmic Surgery. *Invest Ophthalmol Vis Sci*. 2015; 56:3514-. [PubMed: 26030105]
36. Pasricha ND, Shieh C, Carrasco-Zevallos OM, et al. Real-Time Microscope-Integrated OCT to Improve Visualization in DSAEK for Advanced Bullous Keratopathy. *Cornea*. 2015; 34:1606–1610. [PubMed: 26509766]

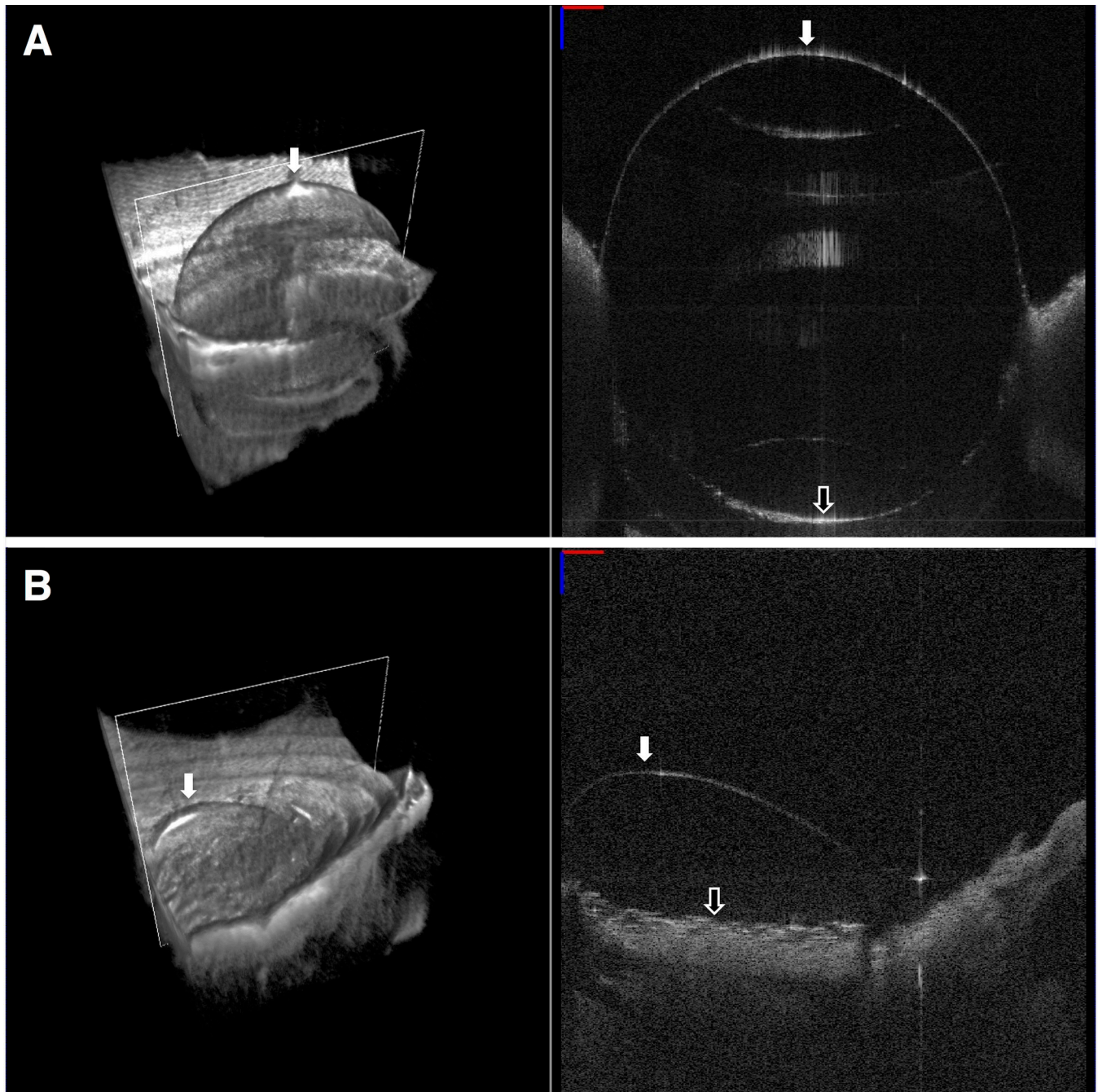


FIGURE 1. Endothelial side up swept-source microscope-integrated optical coherence tomography (SS-MIOCT) images after air injection to confirm big bubble (BB) formation result (Top) Volume (left) and B-scan (right) SS-MIOCT images from a full BB formation group sample showing a single, centrally located bubble >7 mm in diameter (white arrow). The separated corneal stroma (black arrow) could be easily visualized in the B-scan images. (Bottom) Volume (left) and B-scan (right) SS-MIOCT images from a partial BB formation group sample showing a single, peripherally located bubble <7 mm in diameter (white arrow).

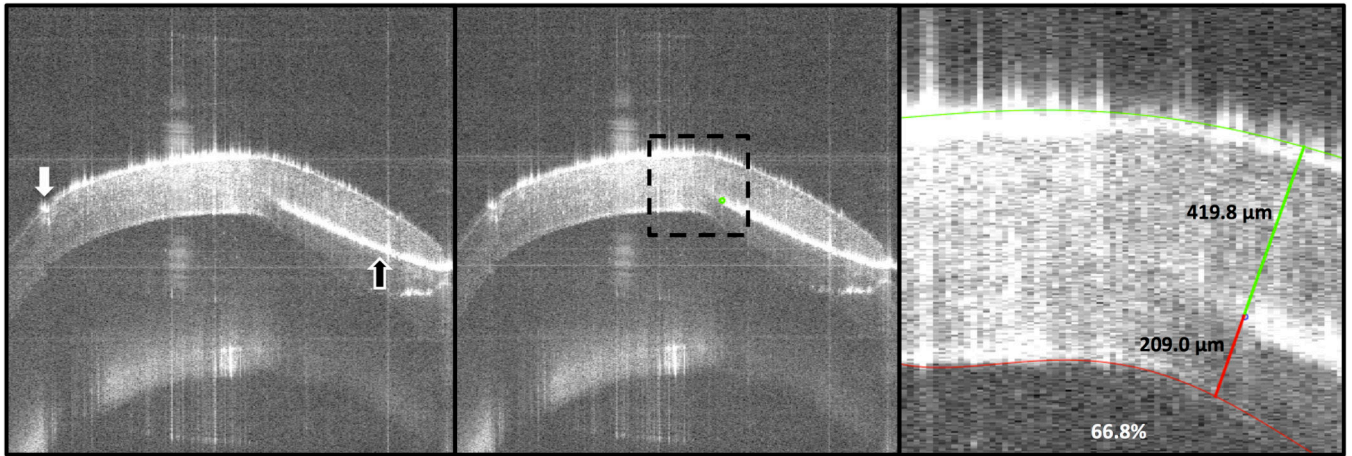


FIGURE 2. Needle depth analysis images for a successful full big bubble (BB) formation group sample

(Left) The paracentral cornea B-scan with the needle (black arrow) tip was selected from the swept-source microscope-integrated optical coherence tomography (SS-MIOCT) volume immediately prior to air injection. The trephination groove (white arrow) could also be visualized. (Center) The needle tip (green dot) was manually segmented and the cornea was cropped to the region of interest (dotted-black box). (Right) The epithelial and endothelial surfaces were semi-automatically segmented. The stroma above the needle (419.8 μm), the stroma below the needle (209.0 μm), and the needle depth percentage (66.8%) were then calculated (numbers refer only to results from this image). The central corneal thickness of this cornea was 501.0 μm .

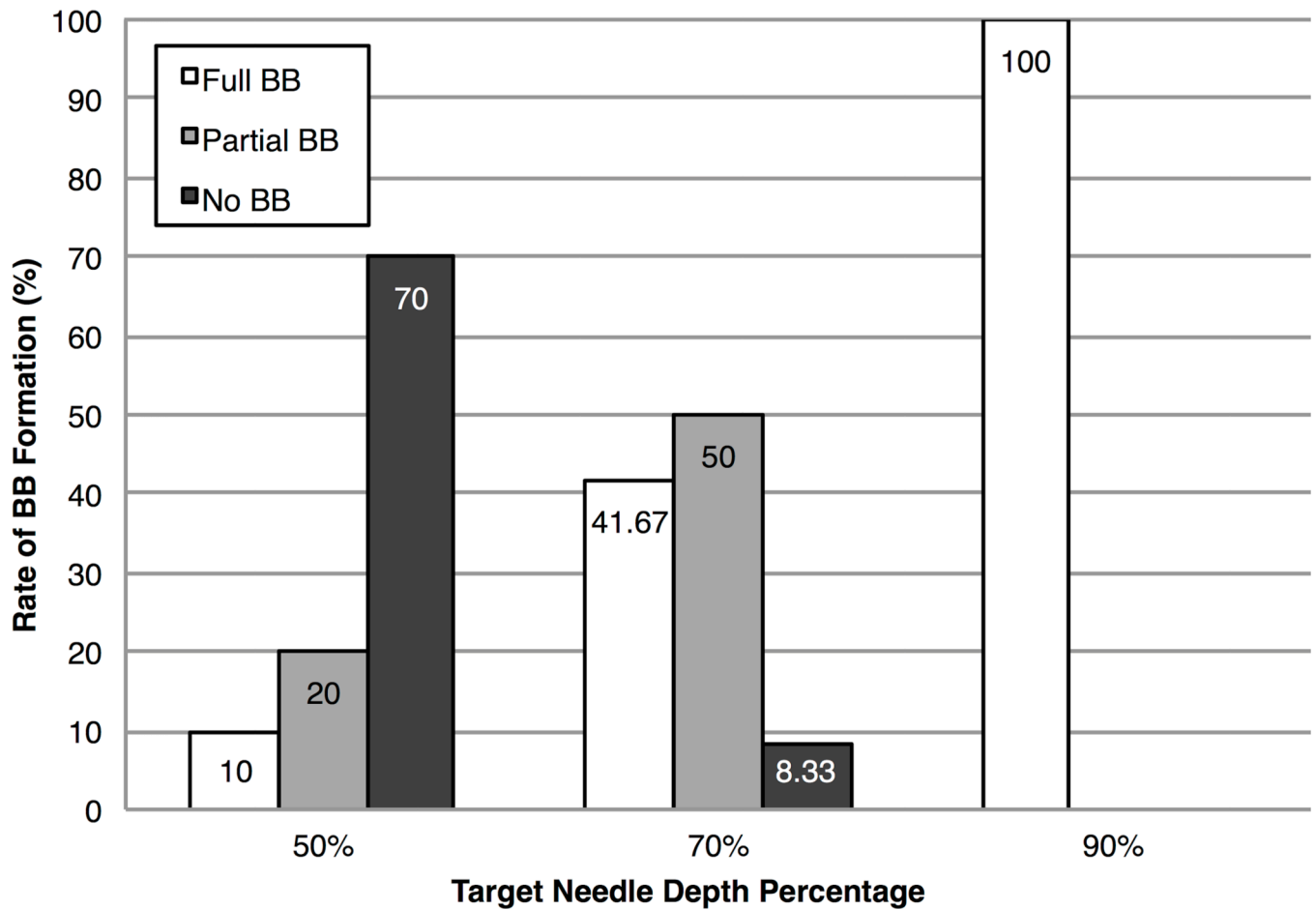


FIGURE 3. Big bubble (BB) formation rates at each target needle depth percentage

Needle injections at a target needle depth of 50% resulted in a majority of unsuccessful no BB formations, whereas those at a target needle depth of 70% resulted in a majority of partial BB formations. All needle injections at a target needle of 90% resulted in successful full BB formations.

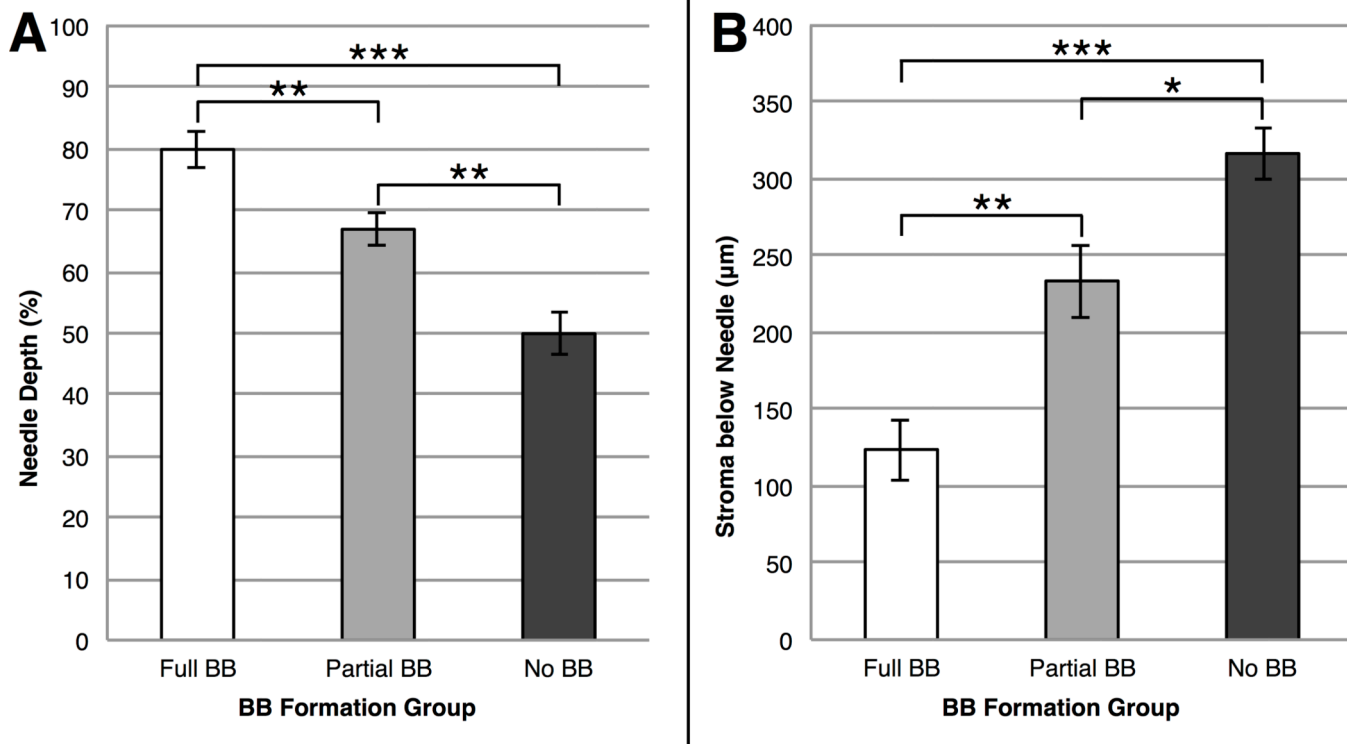


FIGURE 4. Needle depths for each big bubble (BB) outcome
 (Left) Needle depth percentage for the full BB, partial BB, and no BB formation groups. Successful full BB formation required the deepest needle depth percentages followed by partial BB formation and then by no BB formation. (Right) Stroma below needle for the full BB, partial BB, and no BB formation groups. Successful full BB formation had the least stroma below the needle followed by partial BB formation and then by no BB formation. Values are presented as mean±standard error. * = $P<0.05$; ** = $P<0.01$; *** = $P<0.0001$.

TABLE 1

Baseline Characteristics and Needle Insertion Measurements

Measures	Full BB (n=16)	Partial BB (n=8)	No BB (n=8)	P Value*
Males (n)	12 (57.1%)	6 (28.6%)	3 (14.3%)	0.16
Females (n)	4 (36.4%)	2 (18.2%)	5 (45.5%)	
Caucasians (n)	11 (42.3%)	7 (26.9%)	8 (30.8%)	0.08
African Americans (n)	5 (83.3%)	1 (16.7%)	0 (0.0%)	
Age (years)	54.6±3.3	62.5±5.4	62.5±1.7	0.10
ECD (cells/mm ²)	2694±143	2464±280	2317±203	0.37
Air Injected (mL)	2.1±0.3	2.6±0.6	3.6±0.5	0.06
Needle Angle (degrees)	13.8±1.6	12.8±2.6	13.8±1.8	0.93
CCT (µm)	539.3±14.6	588.6±8.5	557.3±21.0	0.11
Stroma Below Needle (µm)	123.9±20.0	233.7±23.8	316.7±17.3	<0.0001
Needle Depth (%)	79.9±3.0	66.9±2.6	49.9±3.4	<0.0001

BB = Big Bubble; ECD = Endothelial Cell Density; CCT = Central Corneal Thickness.

Data are expressed as number (percentage) and mean±standard error.

* Chi-square test for nominal variables and one-way analysis of variance (ANOVA) for continuous variables.